



**HAL**  
open science

# Flux growth synthesis, single crystal and electronic structure of the new intermetallic compound

## **Pt<sub>2</sub>Ga<sub>17</sub>Ta<sub>3</sub>**

Monique Tillard

► **To cite this version:**

Monique Tillard. Flux growth synthesis, single crystal and electronic structure of the new intermetallic compound Pt<sub>2</sub>Ga<sub>17</sub>Ta<sub>3</sub>. Computational Materials Science, 2021, 197, pp.110591. 10.1016/j.commatsci.2021.110591 . hal-03237616

**HAL Id: hal-03237616**

**<https://hal.science/hal-03237616>**

Submitted on 26 May 2021

**HAL** is a multi-disciplinary open access archive for the deposit and dissemination of scientific research documents, whether they are published or not. The documents may come from teaching and research institutions in France or abroad, or from public or private research centers.

L'archive ouverte pluridisciplinaire **HAL**, est destinée au dépôt et à la diffusion de documents scientifiques de niveau recherche, publiés ou non, émanant des établissements d'enseignement et de recherche français ou étrangers, des laboratoires publics ou privés.

# Flux growth synthesis, single crystal and electronic structure of the new intermetallic compound $\text{Pt}_2\text{Ga}_{17}\text{Ta}_3$

Monique Tillard 

ICGM, Univ Montpellier, CNRS, ENSCM, Montpellier, France

E-mail : [monique.tillard@umontpellier.fr](mailto:monique.tillard@umontpellier.fr)

Tel : +33 (0)4 67 14 48 97

 ORCID : 0000-0002-0609-7224

## Abstract

Single crystals of  $\text{Pt}_2\text{Ga}_{17}\text{Ta}_3$  were flux-grown in a high-temperature experiment from a Pt-Ga mixture heated in a sealed tantalum crucible. Typical crystals of this intermetallic compound are hexagonal platelets. The stoichiometry of the compound has been confirmed by energy-dispersive X-ray spectrometry (EDS) and its structure is determined by single-crystal X-ray diffraction at room temperature.  $\text{Pt}_2\text{Ga}_{17}\text{Ta}_3$  crystallizes in a new structural type, with hexagonal symmetry  $P6_3/mmc$  and unit cell of dimensions  $a = 8.1930(4)$ ,  $c = 13.6151(6)$  Å. The structure is described as a packing of polyhedral units, triangular prisms  $\text{Pt}@Ga_6$  and complex units  $\text{Ta}_3@Ga_{20}$  built from three interpenetrating  $\text{Ta}@Ga_{10}\text{Ta}_2$  distorted icosahedra. The compound properties are evaluated from DFT first-principle calculations against those of the In- and Nb- isostructural analogs  $\text{Pt}_2X_{17}M_3$   $X = \text{Ga}, \text{In}$ ,  $M = \text{Ta}, \text{Nb}$ . Results indicate that these compounds are likely to be stable and exhibit similar behavior to  $\text{Pt}_2\text{Ga}_{17}\text{Ta}_3$ , a

compound where binding occurs primarily through metallic interactions despite the presence of localized covalent bonds.

## Keywords

Intermetallics, crystal structure, X-ray diffraction, electronic band structure, flux growth

## 1-Introduction

Among the solid materials, one of the most important classes is that of intermetallic compounds characterized by a great diversity both in terms of their structural chemistry with arrangements most often resulting from 3D compaction and their physical properties ranging from metal to semiconductor due to the complexity of chemical bonding, which mixes metallic and covalent bonds [1-3]. Many devices are made up of metal interfaces and among them, the high frequency or high power semiconductor devices are known to dissipate large amounts of heat causing them to operate at temperatures exceeding sometimes 300 °C. Thus, the metal-semiconductor junction of the widely used Pt/n-GaAs Schottky diode is provided with a thin deposit of platinum. This interface can quickly damage at elevated temperatures, due to reactions between Pt and Ga in the solid-state [4, 5]. Certain surface imperfections have been highlighted by scanning electron and ion microscopies on Pt deposits on GaAs subjected to annealing at 400 °C. The diffusion of Ga from the GaAs substrate into the Pt layer results in the appearance of prominent nodules with a high Ga content, probably related to the formation of an indeterminate compound, rich in Ga, grown in the complex interface [4]. The binary Ga-Pt phase diagram indicates the existence of eight phases or intermetallic compounds:  $\text{GaPt}_3$ ,  $\text{GaPt}_2$ ,  $\text{Ga}_3\text{Pt}_5$ ,  $\text{GaPt}$ ,  $\text{Ga}_3\text{Pt}_2$ ,  $\text{Ga}_2\text{Pt}$ ,  $\text{Ga}_7\text{Pt}_3$  and  $\text{Ga}_6\text{Pt}$  of which the

melting or decomposition temperatures range from 1374 °C ( $\text{GaPt}_3$ ) to 290 °C ( $\text{Ga}_6\text{Pt}$ ) [6-8]. On the other hand, fourteen crystal structures are listed for Ga-Pt binary compounds in Pearson's crystal database [9]. Very recently, the structure of compound  $\text{Ga}_5\text{Pt}$  has been solved and refined from a twinned crystal [10], which constitutes a curious analogy with that of the Al-richest  $\text{Al}_4\text{Pt}$  compound, remained unknown for a long time until its recent structure determination also from a twinned crystal [11]. Considering the particular relationship between the lattice characteristics of  $\text{Ga}_5\text{Pt}$  and the cell parameters given previously for  $\text{Ga}_6\text{Pt}$  as well as the lack of structural determination for  $\text{Ga}_6\text{Pt}$  [12], we have established that  $\text{Ga}_5\text{Pt}$  is the true stoichiometry of the most Ga-rich compound in the system [10].

Besides, several Ta-Ga binary compositions are cited and more or less known from the structural point of view, such as  $\text{TaGa}_2$ ,  $\text{TaGa}_3$ ,  $\text{Ta}_3\text{Ga}_2$ ,  $\text{Ta}_5\text{Ga}_3$ ,  $\text{Ta}_6\text{Ga}_5$  [9] and the recently characterized  $\text{Ta}_4\text{Ga}_5$  compound [13] described with heteroatomic clustering.

During the studies carried out within the binary system Pt-Ga, we serendipitously obtained crystals having a ternary composition. The ability of gallium to promote reactions by acting as a flux had been beneficial to the formation of such a ternary compound by the incorporation of tantalum from the crucible. The study of this ternary intermetallic compound identified as  $\text{Pt}_2\text{Ga}_{17}\text{Ta}_3$  is reported in the current paper that includes the experimental conditions for preparing the compound, the determination and description of its single crystal structure by X-ray diffraction and the evaluation of its properties and those of analogs by a theoretical DFT approach.

## 2. Experimental section

### 2.1 *Synthesis*

The ternary compound was obtained for the first time during the preparation of a binary compound starting with a mixture with the nominal composition  $\text{Ga}_4\text{Pt}$  heated to 973 K in a tantalum tube, weld-sealed under argon and protected inside a stainless steel jacket. In this experiment, the metallic elements Pt (foil, Aldrich, 99.99%) and Ga (Rhône Poulenc, 6N) were taken without further purification. An accidental interruption of unknown duration followed by a restart of the heating program altered the thermal history of this sample and led to the formation of  $\text{Pt}_2\text{Ga}_{17}\text{Ta}_3$  crystals. Alloying Pt and Ga in a conventional furnace for compositions rich in gallium is affordable despite the difference in their melting points (303 K for Ga and 2041 K for Pt) because gallium acts as a flux. This is the reason why Ta ( $T_f = 3290$  K) from the crucible could enter the composition. The flux-grown crystals shown in Figure 1 display well-defined faces with sharp edges and hexagonal shapes. Later, this ternary compound was prepared again in an arc furnace experiment and easily obtained by reacting Ta powder (Aldrich, 99.9%) with a stoichiometric amount of Pt and a very slight excess of Ga to compensate for possible evaporation losses. The individualized crystals then extracted from the top of the ingot were found to have the same stoichiometry as the crystals previously obtained by chance.

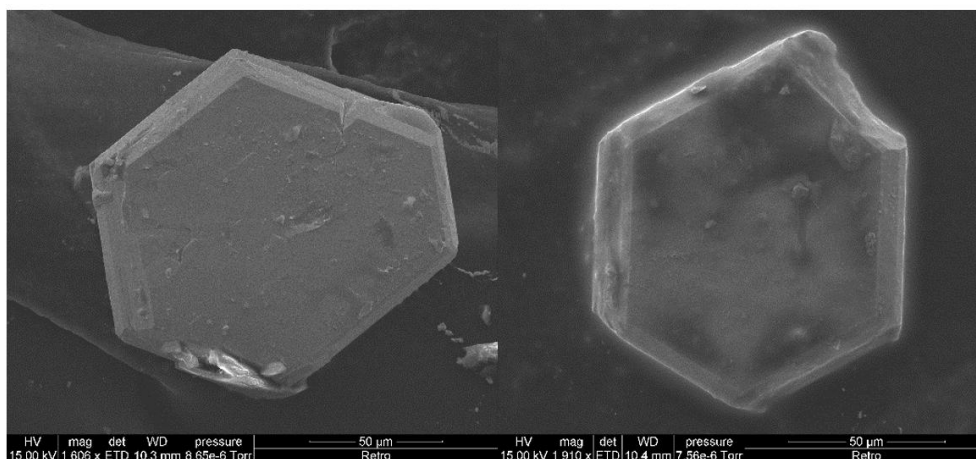


Figure 1. Typical flux-grown single crystals of  $\text{Pt}_2\text{Ga}_{17}\text{Ta}_3$

## 2.2 *X-ray diffraction and EDX analysis*

The best diffracting single crystal was selected to collect the X-ray diffracted intensities at room temperature using an Xcalibur CCD (Oxford Diffraction) four-circle diffractometer equipped with a Mo  $K\alpha$  source. The data were corrected for Lorentz-polarization effects using the 'multi-scan' procedure included in CrysAlis software [14]. The structure was solved by direct methods and refined by full-matrix least-squares using SHELX programs [15]. The free refinement of the site occupation factors indicating no variation confirmed the total filling of the sites. In the final refinements, anisotropic displacement parameters were considered for all the atoms. The chemical composition of the crystals was checked by classical EDX analyses performed on an Oxford Instrument Environmental Scanning Electron Microscope, equipped with an X-Max large area SDD sensor that allows excellent sensitivity/precision/resolution. The absence of significant variation in the stoichiometry when scanning across their surface proved the good homogeneity of the samples. **Pt:Ga:Ta** were detected in the respective atomic percentages **8.5(2):77.2(2):14.3(2)**, which is in very

good agreement with  $\text{Pt}_2\text{Ga}_{17}\text{Ta}_3$ , the formula established by the X-ray structural determination.

### 2.3 Computational details and method

The calculations were carried out using the DFT plane-wave pseudo-potential method provided in the program CASTEP [16]. The exchange-correlation energy was evaluated using the generalized gradient approximation GGA and the PW91 gradient-corrected functional [17]. Ultra-soft USPP pseudopotentials [18] were selected with a density-mixing scheme for BFGS geometry optimizations. Pt ( $5d^9, 6s^1$ ), Ta ( $5d^3, 6s^2$ ), Nb ( $4s^2, 4p^6, 4d^4, 5s^1$ ), Ga ( $3d^{10}, 4s^2, 4p^1$ ) and In ( $4d^{10}, 5s^2, 5p^1$ ) were considered as valence states. The electronic wave functions were expanded to kinetic energy cut-offs set at the ultrafine quality level and Monkhorst–Pack grids of generated k-points [19] were used for sampling of the Brillouin zone. The lattice parameters and the atomic positions have been fully relaxed in the calculations, with tolerance limits fixed to  $5 \times 10^{-6}$  eV/atom for the total energy, 0.01 eV/Å for the forces and  $5 \times 10^{-4}$  Å for the atomic displacements.

## 3- Crystal structure

As suggested by the shape of the crystals, hexagon-like platelets selected for intensity measurements, the diffraction data conforms to the hexagonal symmetry. Moreover, the  $hhl$  reflections with  $l = 2n+1$  were systematically absent from the dataset indicating the  $P6_3/mmc$  space group. Thus, the reflections were indexed accordingly in this space group with a hexagonal cell of dimensions  $a = 8.1930(4)$ ,  $c = 13.6151(6)$  Å. The main parameters related to crystal, data collection and structural refinement are given in Table 1.

Table 1. Crystal data and structure refinement for  $\text{Pt}_2\text{Ga}_{17}\text{Ta}_3$

Temperature	293(2) K
Symmetry, space group	hexagonal, $P6_3/mmc$ (N°. 194)
Unit cell dimensions	$a = 8.1947(2)$ , $c = 13.6159(6)$ Å
<b>Z</b>	<b>2</b>
Calculated density	8.884 Mg/m <sup>3</sup>
Radiation, wavelength	Mo K $\alpha$ , 0.71073 Å
Crystal size	0.10 × 0.14 × 0.03 mm <sup>3</sup>
Absorption coefficient	66.528 mm <sup>-1</sup>
$\theta$ range	3.237 to 32.686 °
Collected / independent reflections	19407 / 587 [Rint = 0.1415]
Goodness-of-fit on F <sup>2</sup>	1.185
Final R indices [ $I > 2\sigma(I)$ ]	R1 = 0.0419, wR2 = 0.0999
R indices (all data)	R1 = 0.0589, wR2 = 0.1048
Largest diff. peak and hole	5.17 and -2.88 e.Å <sup>-3</sup>

The structural atomic model is built with six independent atoms at special symmetry positions. Ta atom is placed at a  $6h$  position ( $x, 2x, 1/4$ ; symmetry  $mm$ ), Pt at a  $4f$  position ( $1/3, 2/3, z$ ; symmetry  $3m$ ) and Ga is distributed over four distinct sites: one  $4e$  ( $0, 0, z$ ; symmetry  $3m$ ), one  $6h$  and two  $12k$  ( $x, 2x, z$ ; symmetry  $m$ ). When this structural model corresponding to the formula  $Pt_2Ga_{17}Ta_3$  is refined with anisotropic displacement parameters for all the atoms, the final agreement R1 factor converges to 4.19%. The structural data are reported in Table 2, the final atomic coordinates **have been standardized using StructureTIDY [20]** and equivalent isotropic displacement parameters are given. The full CIF file deposited at the Cambridge Crystallographic Data Center (CCDC) [21] can be freely obtained by providing the CSD number **2068742**.

Table 2. Atomic coordinates and equivalent displacement parameters ( $\text{Å}^2 \times 10^3$ )

Atom	site	x	y	z	$U_{eq}$
------	------	---	---	---	----------

Ta	$6h$	0.1224(1)	0.2449(1)	1/4	7(1)
Pt	$4f$	1/3	2/3	0.5420(1)	8(1)
Ga1	$12k$	0.1935(1)	0.3870(3)	0.6449(1)	14(1)
Ga2	$12k$	0.2040(1)	0.4081(3)	0.0754(2)	17(1)
Ga3	$6h$	0.4549(2)	0.9098(4)	1/4	14(1)
Ga4	$4e$	0	0	0.0898(3)	13(1)

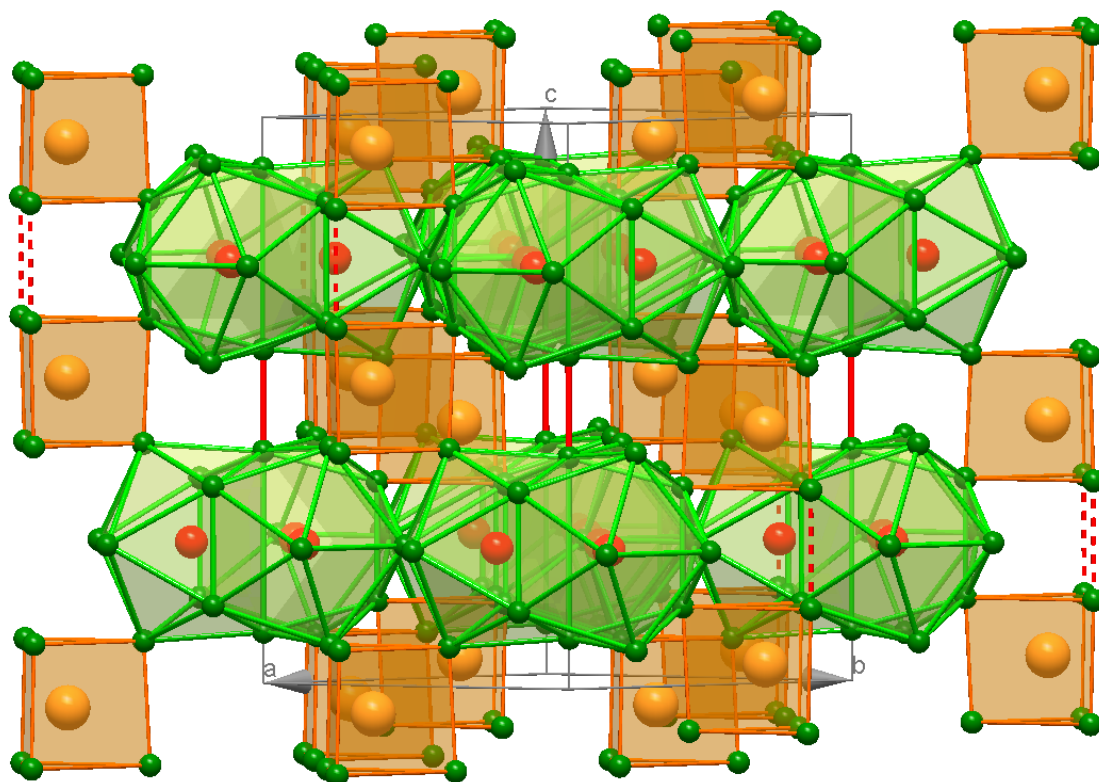


Figure 2. Three-dimensional packing in hexagonal  $\text{Pt}_2\text{Ga}_{17}\text{Ta}_3$  highlighting the coordination polyhedra: complex  $\text{Ta}_3@ \text{Ga}_{20}$  units (green) around Ta atoms (red spheres) at  $z = 1/4, 3/4$  and triangular prisms  $\text{Pt}@ \text{Ga}_6$  (orange) around Pt atoms (large orange spheres) at  $z = 0, 1/2$ . The Ga atoms are drawn as small green spheres.

The hexagonal crystal structure of  $\text{Pt}_2\text{Ga}_{17}\text{Ta}_3$  could be described as a close-packed three-dimensional arrangement of atoms, but it is easier to visualize by considering the polyhedral coordination shells around each type of atom as represented in Figure 2.

Each Pt atom is surrounded by six Ga atoms distant from  $\sim 2.43 \text{ \AA}$  ( $3 \times \text{Ga1}$  and  $3 \times \text{Ga2}$ ), at vertices of a triangular prism displaying the  $3m$  symmetry. These  $\text{Pt@Ga}_6$  polyhedra occur along the  $c$ -axis approximately at  $z = 0$  and  $z = \frac{1}{2}$  and share their vertices with six Ta-centered neighboring units. The Ta atoms of the structure are placed at the intermediate levels  $z = \frac{1}{4}$  and  $z = \frac{3}{4}$  and their closest neighbors are gallium atoms:  $2 \times \text{Ga3}$  at  $2.60 \text{ \AA}$ ,  $2 \times \text{Ga2}$  at  $2.64 \text{ \AA}$ ,  $2 \times \text{Ga4}$  at  $2.78 \text{ \AA}$  and  $4 \times \text{Ga1}$  at  $2.80 \text{ \AA}$ . Two additional Ta neighbors located at  $3.01 \text{ \AA}$  complete this surrounding shell to form a distorted  $\text{Ga}_{10}\text{Ta}_2$  icosahedron having only  $m$  symmetry. Each  $\text{Ta@Ga}_{10}\text{Ta}_2$  polyhedron thus formed (blue icosahedra in Figure 3) shares its two Ga3 vertices with two similar units. Since Ta is on a unique independent crystallographic position ( $6h$ ), all the Ta atoms in this structure are equivalent. They are therefore at the center and on the surface of these  $\text{Ta@Ga}_{10}\text{Ta}_2$  units. For the structural description, it is then preferable to consider larger triple-units (shown as green polyhedra in Figure 3), made of three collapsed/interpenetrated icosahedra, which incorporate in their center a triangle  $\text{Ta}_3$ . The Ta-Ta distance of  $3.01 \text{ \AA}$  **within these triangles is comparable to the distances measured in  $\text{Ta}_4\text{Ga}_5$  in which the significant contribution of Ta-Ta bonding has been demonstrated [13]**. It becomes easy to describe the structural packing in terms of regular alternation along the  $c$ -axis of layers with such  $\text{Ta}_3\text{@Ga}_{20}$  collapsed tri-icosahedra and layers with  $\text{Pt@Ga}_6$  prisms. These two kinds of layers are interconnected *via* vertex-sharing of their respective constituent polyhedra but it is important to note that direct links are also established between polyhedral units belonging to successive layers of the same nature. The  $\text{Ta}_3\text{@Ga}_{20}$  units are interconnected by Ga4-Ga4 bonds of  $2.45 \text{ \AA}$  (red solid lines in Figure 3) which are

significantly shorter than the following distances of 2.84 Å at the common Ga1-Ga4 edges of Ta@Ga<sub>10</sub>Ta<sub>2</sub> icosahedra (see in Figure 4) and 2.87 Å at the Ga1-Ga1 links between Pt@Ga<sub>6</sub> prisms belonging to successive layers (red dashed lines in Figure 3).

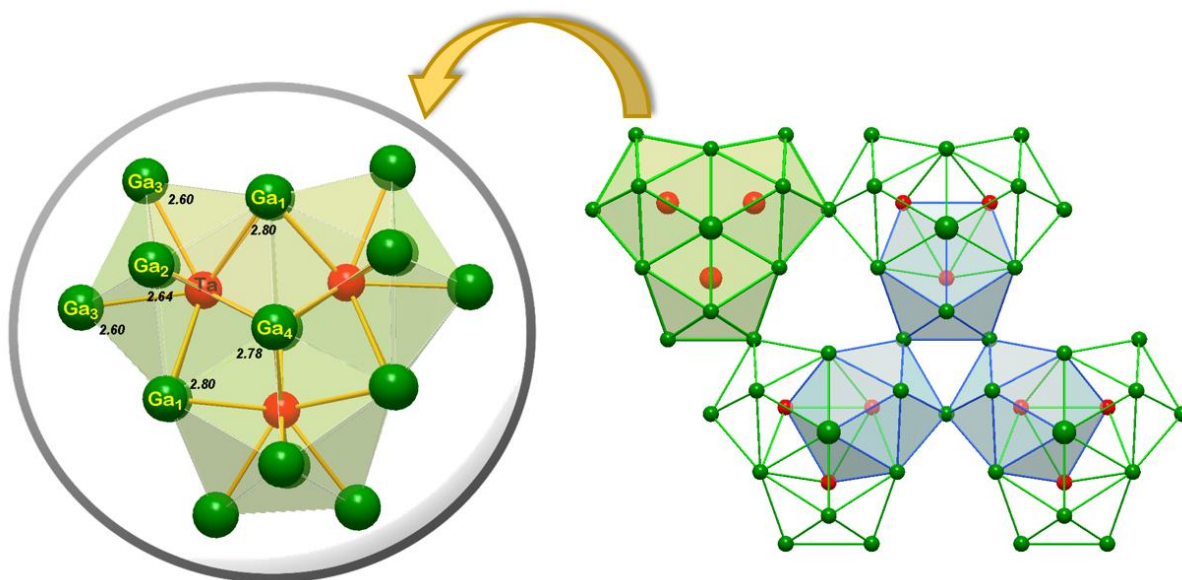


Figure 3. The Ta-centered icosahedra Ta@Ga<sub>10</sub>Ta<sub>2</sub> (blue filled polyhedra) combine 3 by 3 in collapsed/ interpenetrated Ta<sub>3</sub>@Ga<sub>20</sub> units (green filled polyhedra) enclosing a Ta<sub>3</sub> triangle (red spheres) and sharing Ga vertices with similar units. The numbers printed close to the Ga atoms give their distance in Å to the Ta centers.

It is appropriate to comment on the interatomic distances to avoid any misunderstanding of the atom arrangement in this structure. Gallium, like other triels, is known as an icosogenic element due to its ability to generate icosahedra in its intermetallic combinations [22]. Therefore, numerous arrangements in the intermetallic phases of gallium have been described in terms of gallium icosahedral clusters. This is particularly true for the phases formed with electropositive (alkaline) elements that belong to the family of Zintl compounds [1, 23, 24]. Bonding therein is interpreted using both the concept of localized bonding with  $2c-2e$  classical covalent Ga-Ga bonds ( $\sim 2.4-2.5\text{\AA}$ ) between polyhedra, and the notion of locally

delocalized bonding with elongated and electron-deficient Ga-Ga bonds ( $\sim 2.7$  Å) at icosahedra edges [23, 25]. In the structure of  $\text{Pt}_2\text{Ga}_{17}\text{Ta}_3$  reported here, short classical Ga-Ga covalent bonding (2.445 Å) can be pointed out between the tri-icosahedral units. **Similar short and even shorter classical covalent bonds between Ga atoms are reported in intermetallic or organometallic compounds** [26-29]. However, the situation differs somewhat within the polyhedra with much longer Ga-Ga edges of 2.8 to 3.0 Å. Given the Ga covalent radius of 1.26 Å, so long interatomic distances can no longer be considered as really binding covalent interactions, even of the delocalized type. Therefore, we must keep in mind that the interpretation in terms of polyhedra is convenient to facilitate the description of the structural arrangement and make it easier to understand. Another, not necessarily more realistic, description of bonding could be provided by the comparison of the experimental interatomic distances to the sum of covalent radii of the elements (1.37 and 1.43 Å for Pt and Ta, respectively). In addition to the above-mentioned Ga-Ga bond of 2.45 Å, this leads to consider quite strong Pt-Ga and Ta-Ga covalent bonds of 2.43 and 2.60 Å, as their lengths are shorter than the sum of the covalent radii of the atoms.

**The question of the interpretation of bonding and thus the classification of this compound may then arise. Whatever its classification, both concepts of multicenter delocalized and classical localized  $2c-2e$  bonding should be used to describe this structure. The Zintl concept would necessarily imply considering Ta as an electropositive element, which transfers electrons to stabilize an anionic lattice. In addition, simple methods of counting electrons such as skeletal polyhedral electron pairs (PSEPT) could have been useful in understanding the aggregation and bonding. Nevertheless, they are not so easy to apply to the collapsed units in this structure that are Ta- or Pt-centered and share most of their vertices. With the presence of such condensed units and an  $e/a$  count of 2.7, the compound  $\text{Pt}_2\text{Ga}_{17}\text{Ta}_3$  is characterized by**

an "electron deficit" and enters the  $e/a$  scale in an intermediate domain between the Hume Rothery and Zintl phases, that of polar intermetallic phases [30]. The review dedicated to the large family of intermetallic polar compounds classifies them in two main categories, either with poly-cationic clusters surrounded by anionic ligands or poly-anionic units combined with monoatomic cations [30]. It highlights the main aspects to take into account for the interpretation of such complex compounds but concludes that the real nature of the bonding requires an inspection, on a case-by-case basis, of their electronic structures.

#### 4- DFT analysis

A theoretical approach seems useful to help understand this new ordered intermetallic compound and provide additional information not only on bonding but also on the properties expected for  $\text{Pt}_2\text{Ga}_{17}\text{Ta}_3$ . Starting with its experimental structure, accurate optimized geometry was obtained in the DFT calculations by completely relaxing the lattice parameters and the atom positions. The dimensions of the optimized cell did not vary by more than 2% from the experimental values, both for  $\text{Pt}_2\text{Ga}_{17}\text{Ta}_3$  and for the hypothetical isostructural compound  $\text{Pt}_2\text{Ga}_{17}\text{Nb}_3$  resulting from the replacement of Ta by Nb. The supplemental changing of Ga for In leads to the isostructural models  $\text{Pt}_2\text{In}_{17}\text{Ta}_3$  and  $\text{Pt}_2\text{In}_{17}\text{Nb}_3$  for which the optimized cell parameters are elongated by  $\sim 9\%$  after geometry optimization. The increase in the atomic radii from Ga to In, from 1.30 to 1.55 Å, accounts for such an expansion of the cell volume.

A first look at the enthalpy of formation of these experimental and hypothetical compounds can provide a rough estimate of their stability. This quantity is defined as  $\Delta H_f = E_{\text{tot}}(\text{A}_x\text{B}_y\text{C}_z) - x \times E_{\text{tot}}(\text{A}) - y \times E_{\text{tot}}(\text{B}) - z \times E_{\text{tot}}(\text{C})$  *i.e.* as the difference in the computed total energies between the compound and its constitutive elements taken in their solid-state structures.

These solid-state structures, listed in Table 3, were optimized in the same conditions as the structures of compounds.

Table 3. Lattice parameters of the elements in their solid-state structures

	System	Space group	lattice parameters (Å)
Ta	cubic	Fm $\bar{3}$ m	a = 2.862
Pt	cubic	Fm $\bar{3}$ m	a = 3.931
Nb	cubic	Im $\bar{3}$ m	a = 3.297
In	tetragonal	I4/mmm	a = 3.253, c = 4.946
Ga	Orthorhombic	Cmca	a = 4.523, b = 7.661, c = 4.524

The negative values calculated for the enthalpy of formation of the four compounds indicate that such intermetallic combinations can form with the current atomic arrangement. The values of the enthalpy per atom,  $\Delta H_{f/atom}$  -0.31 eV/atom for Pt<sub>2</sub>Ga<sub>17</sub>Ta<sub>3</sub>, -0.33 eV/atom for Pt<sub>2</sub>Ga<sub>17</sub>Nb<sub>3</sub>, -0.14 eV/atom for Pt<sub>2</sub>In<sub>17</sub>Nb<sub>3</sub> and -0.12 eV/atom for Pt<sub>2</sub>In<sub>17</sub>Ta<sub>3</sub>, remain of the same order of magnitude. Although their direct comparison is quite tricky, the higher negative values associated with the gallium compounds should be underlined, suggesting that they are probably the easiest to form.

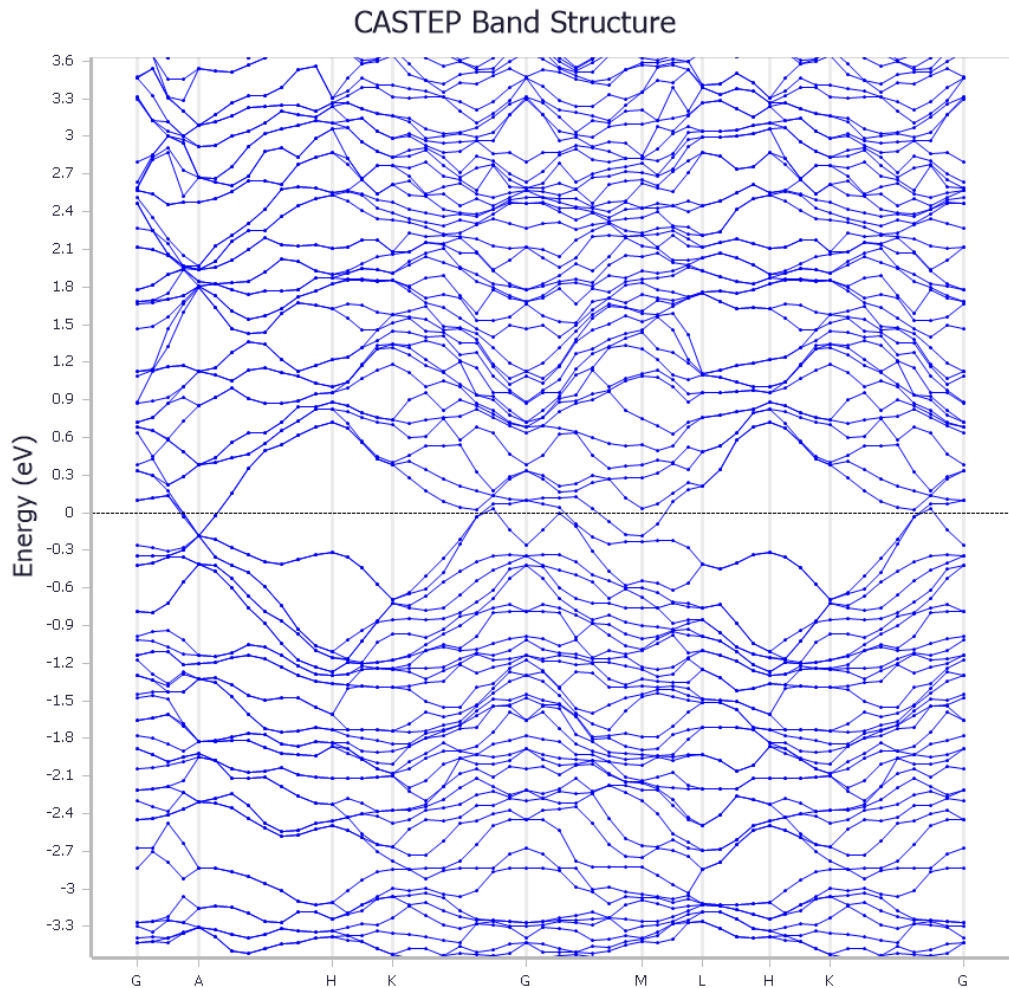


Figure 4. Dispersion curves calculated for  $\text{Pt}_2\text{Ga}_{17}\text{Ta}_3$  (CASTEP code)

The dispersion curves plotted for  $\text{Pt}_2\text{Ga}_{17}\text{Ta}_3$  along the usual representative paths in the Brillouin zone of a hexagonal compound are given in Figure 4. The band structures calculated for the other three compounds are very similar, with not very dispersive bands that cross the Fermi level in all segments except H→K and H→L. This is in good agreement with the metallic character that can be expected for these compounds.

The total density of states, DOS, as well as its partial atomic contributions, PDOS, are also useful quantities to provide an informative description of the structures. With a deep valley between the bonding and antibonding states, the general shape of the DOS curves shows great

similarities for the four compounds. The Fermi energy lies at the bottom of narrow pseudo gaps of about 0.2-0.3 eV, conferring these compounds certain stability since their bonding/valence band is almost entirely filled by electrons, while their antibonding/conduction band remains almost empty.

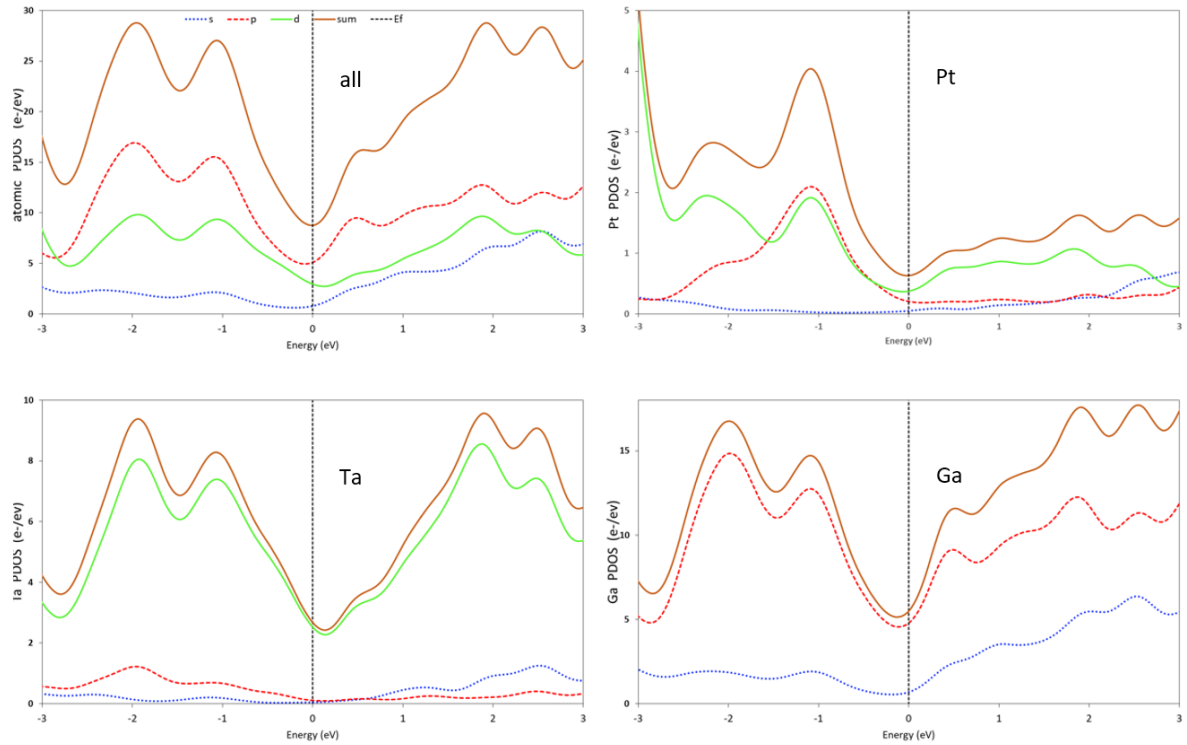


Figure 5. Partial PDOS and total DOS for all atoms *top left*, Pt *top right*, Ta *bottom left*, and Ga *bottom right*. Blue dotted lines represent the contribution of the *s* states, red dotted lines the contribution of the *p* states, solid green lines the contribution of the *d* states and solid brown lines the total density.

A careful examination of the partial atomic PDOS is also relevant to obtain additional information, particularly in the Fermi level region where occur the levels, most often a limited number of levels, that typically govern the transport properties of compounds. For the

compounds  $\text{Pt}_2\text{X}_{17}\text{M}_3$  investigated in this study, it comes that all of the  $s$ ,  $p$  and  $d$  states contribute significantly to the total DOS in the whole energy domain, indicating a high degree of mixing (hybridization) of the atomic levels. As seen in Figure 4, this is especially true at energies close to the Fermi energy even if the contribution of Pt atoms is more marked in the bonding domain than above the Fermi level. These are the  $X$  atoms, Ga or In, that participate the most in the total density, primarily *via* their  $p$  states as shown by the Ga PDOS curves represented in Figure 5. Although to a lesser extent, the strong contribution of the  $nd$  states of  $M$  (Ta or Nb) atoms suggests the role the nature of the  $M$  element might play.

The distribution of the metallic states is quite similar for Ga or In compounds but differs slightly so that the total density of states at the Fermi level of about  $9 \text{ e}^-/\text{eV}$  in Ga compounds, reaches more than  $12 \text{ e}^-/\text{eV}$  when  $X$  is indium. The comparison of PDOS at Fermi level for compounds  $\text{Pt}_2\text{Ga}_{17}\text{Ta}_3$  and  $\text{Pt}_2\text{In}_{17}\text{Ta}_3$  tells that  $X$  (Ga or In) contribution is highly dominated by the  $p$  states,  $4.7 \text{ e}^-$  in the case of Ga and  $6.0 \text{ e}^-$  in the case of In. Similarly, the contribution of Pt that mainly involves the  $d$  (60%) and  $p$  states is higher in the In compound than in the Ga compound ( $0.8 \text{ vs. } 0.6 \text{ e}^-$ ). For both compounds, the participation of Ta atoms of about  $4.5 \text{ e}^-/\text{eV}$  is mostly dominated by the  $d$  states.

All the elements gained from partial and total DOS analysis are fully consistent with both the calculated enthalpies of formation and the metallic character found for the compounds. They also highlight the potential role of the nature of the  $X$  atoms (Ga or In) on the electronic properties of the compounds.

Another quantity also accessible from the calculations is the difference in electron density, which is a convenient and valuable tool in the analysis of the properties of compounds. Computed as the density of isolated atoms subtracted from the total electron density, it may provide a graphical visualization of the bonding.

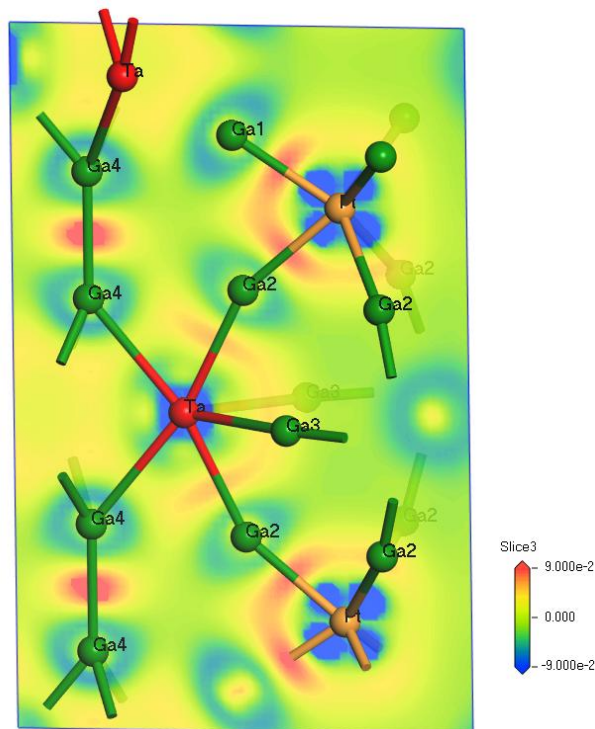


Figure 6. Electron density difference map computed for Pt<sub>2</sub>Ga<sub>17</sub>Ta<sub>3</sub>, shown approximately in the (2 1 0) plane. The highest positive densities (red), especially at Ga4-Ga4 pairs, account for bond formation while negative (blue) densities are a sign of electron loss.

At first glance, the electron density difference map produced for Pt<sub>2</sub>Ga<sub>17</sub>Ta<sub>3</sub> and given in Figure 4 is characterized by a fairly diffuse electron density between all atoms, in agreement with a global metallic character. Yet, some details deserve to be stressed, as the presence of highly positive zones, especially at Ga4-Ga4 "inter-polyhedral" links. Such a high density indicates the existence of interatomic bonds with a rather "strong" covalent character in this compound where bonding mainly proceeds through metallic interactions. These maps also allow visualizing the covalent links of Ga atoms to the Ta and Pt centers while the density is rather low between the Ga atoms at the surface of polyhedra. These elements in a way validate the structural description of these compounds assumed to behave as metallic

conductors in terms of polyhedra interconnected by covalent bonds within a three-dimensional network.

## Conclusion

The new intermetallic compound  $\text{Pt}_2\text{Ga}_{17}\text{Ta}_3$  first obtained by hazard has been prepared from the elements. Its hexagonal structure determined by single-crystal X-ray diffraction at room temperature is described in terms of interconnected polyhedral units packed within a three-dimensional network. A theoretical DFT approach brings proof that isostructural homologs with indium and niobium may exist. They are expected, as  $\text{Pt}_2\text{Ga}_{17}\text{Ta}_3$ , to display some localized covalent bonding and to behave as metallic conductors. [https://doi-org.inc.bib.cnrs.fr/10.1016/0079-6786\(93\)90001-8](https://doi-org.inc.bib.cnrs.fr/10.1016/0079-6786(93)90001-8)

## References

- [1] - C. Belin and M. Tillard-Charbonnel, *Frameworks of Clusters in Alkali-Metal Gallium Phases. Structure, Bonding and Properties.*, Prog. Solid State Chem. 22 (1993) pp. 59-109  
doi: 10.1016/0079-6786(93)90001-8
- [2] - J. Dshemuchadse and W. Steurer, *More of the "Fullercages"*, Z. Anorg. Allg. Chem. 640 (2014) pp. 693-700  
doi: 10.1002/zaac.201300629
- [3] - A. Ovchinnikov, V. Smetana, and A.-V. Mudring, *Metallic alloys at the edge of complexity: structural aspects, chemical bonding and physical properties*, J. Phys. Condens. Mat. 32 (2020) pp. 243002  
doi: 10.1088/1361-648x/ab6b87
- [4] - D.L. Begley, R.W. Alexander, R.J. Bell, and C.A. Goben, *Reaction at a platinum-gallium arsenide interface*, Surface Sci. 104 (1981) pp. 341-353  
doi: 10.1016/0039-6028(81)90064-9
- [5] - C.C. Chang, S.P. Murarka, V. Kumar, and G. Quintana, *Interdiffusions in thin-film Au on Pt on GaAs (100) studied with Auger spectroscopy* J. Appl. Phys. 46 (1975) pp. 4237  
doi: 10.1063/1.321406

- [6] - P. Guex and P. Feschotte, *Les systèmes binaires platine-aluminium, platine-gallium et platine-indium*, J. Less Common Met. 46 (1976) pp. 101-116
- [7] - M. Li, C. Li, F. Wang, and W. Zhang, *Thermodynamic assessment of the Ga-Pt system*, Intermetallics 14 (2006) pp. 826-831  
doi: 10.1016/j.intermet.2005.12.002
- [8] - B.C. Giessen, R.H. Kane, and N.J. Grant, *On the Constitution Diagram Ta-Pt Between 50-100 At. % Pt*, Trans. Metall. Soc. AIME 233 (1965) pp. 855-864
- [9] - P. Villars and K. Cenzual, *Pearson's Crystal Data: Crystal Structure Database for Inorganic Compounds*, ASM International, Materials Park, Ohio, USA (Release 2009/10)
- [10] - M. Tillard and C. Belin, *The new intermetallic compound Ga<sub>5</sub>Pt: Structure from a twinned crystal*, Intermetallics 19 (2011) pp. 518-525  
doi: 10.1016/j.intermet.2010.11.031
- [11] - M. Wörle, F. Krumeich, T. Chatterji, S. Kek, and R. Nesper, *On the structure and twinning of PtAl<sub>4</sub>*, J. Alloys Compd. 455 (2008) pp. 130-136  
doi: 10.1016/j.jallcom.2007.01.161
- [12] - S. Bhan and K. Schubert, *Zum Aufbau der System Kobalt-Germanium, Rhodium-Silizium sowie einiger verwandter Legierungen*, Z. Metallkd. 51 (1960) pp. 327-339
- [13] - R.T. Fredrickson, B.J. Kilduff, and D.C. Fredrickson, *Homoatomic Clustering in T<sub>4</sub>Ga<sub>5</sub> (T = Ta, Nb, Ta/Mo): A Story of Reluctant Intermetallics Crystallizing in a New Binary Structure Type*, Inorganic Chemistry 54 (2015) pp. 821-831  
doi: 10.1021/ic501966v
- [14] - CrysAlis'Red' 171 software package, Oxford diffraction Ltd, Abingdon, United Kingdom. (2004)
- [15] - G.M. Sheldrick, *Crystal structure refinement with SHELXL*, Acta Cryst. C71 (1997) pp. 3-8
- [16] - S.J. Clark, M.D. Segall, C.J. Pickard, P.J. Hasnip, M.J. Probert, K. Refson, and M.C. Payne, *First principles methods using CASTEP*, Z. Kristallog. 220 (2005) pp. 567-570  
doi: 10.1524/zkri.220.5.567.65075
- [17] - J.P. Perdew, J.A. Chevary, S.H. Vosko, M.R. Pederson, D.J. Singh, and C. Fiolhais, *Atoms, molecules, solids, and surfaces: Applications of the generalized gradient approximation for exchange and correlation*, Phys. Rev. B 46 (1992) pp. 6671

doi: 10.1103/PhysRevB.46.6671

[18] - D. Vanderbilt, *Soft self-consistent pseudopotentials in a generalized eigenvalue formalism.*, Phys. Rev. B 41 (1990) pp. 7892-7895

doi: 10.1103/PhysRevB.41.7892

[19] - H.J. Monkhorst and J.D. Pack, "*Special points for Brillouin-zone integrations*"—a reply, Phys. Rev. B 16 (1997) pp. 1748

doi: 10.1103/PhysRevB.16.1748

[20] - L.M. Gelato and E. Parthé, *STRUCTURE TIDY - a computer program to standardize crystal structure data*, J. Appl. Cryst. 20 (1987) pp. 139-143

[21] - <http://www.ccdc.cam.ac.uk/conts/retrieving.html> (or from the CCDC, 12 Union Road, Cambridge CB2 1EZ, UK; Fax: +44 1223 336033; E-mail: deposit@ccdc.cam.ac.uk). Available at. Accessed on.

[22] - R.B. King, *Metal cluster topology. 10. Polyhedral gallium cluster anions in intermetallic phases of gallium and alkali metals*, Inorg. Chem. 28 (1989) pp. 2796-2799

doi: 10.1021/ic00313a021

[23] - C. Belin and M. Tillard-Charbonnel, *Aspects of anionic framework formation. Clustering of p-block elements*, Coord. Chem. Rev. 180 (1998) pp. 529-564

doi: 10.1002/CHIN.199912266

[24] - S.M. Kauzlarich, *Special Issue: Advances in Zintl Phases*, Materials 12 (2019) pp. 2554

doi: 10.3390/ma12162554

[25] - M. Tillard-Charbonnel, A. Manteghetti, and C. Belin, *Icosahedron oligomerization and condensation in intermetallic compounds. Bonding and electronic requirements*, Inorg. Chem. 39 (2000) pp. 1684-1696

doi: 10.1021/ic9910817

[26] - L. R.G. and B. C., *Structure of the Intermetallic Compound Na<sub>22</sub>Ga<sub>39</sub> (~36.07% Na)*, Acta Cryst. B38 (1982) pp. 1101-1104

[27] - J.H.N. Van Vucht, *On the crystal structures of some compounds of gallium with potassium, rubidium and caesium*, Journal of the Less Common Metals 108 (1985) pp. 163-175

doi: [10.1016/0022-5088\(85\)90440-0](https://doi.org/10.1016/0022-5088(85)90440-0)

[28] - W. Uhl, T. Spies, and R. Koch, *Di( $\mu$ -acetato)dialkyldigallium as starting compound for the facile syntheses of digallium derivatives containing bridged or terminally co-ordinated Ga–Ga single bonds*, Journal of the Chemical Society, Dalton Transactions (1999) pp. 2385-2392

doi: 10.1039/A903437D

[29] - P. Wei, X.-W. Li, and G. H. Robinson, *[Ga<sub>2</sub>Cl<sub>4</sub>(dioxane)<sub>2</sub>]: molecular structure and reactivity of a polymeric gallium(II) halide containing two five-coordinate gallium atoms about a Ga–Ga bond*, *Chemical Communications* (1999) pp. 1287-1288  
doi: 10.1039/A903166I

[30] - F. Gladisch and S. Steinberg, *Revealing Tendencies in the Electronic Structures of Polar Intermetallic Compounds*, *Crystals* 8 (2018) pp. 80  
doi: 10.3390/cryst8020080